Improving the Transparency of Stretched Poly(ethylene terephthalate)/Polyamide Blends

V. Prattipati,[1] Y. S. Hu,[1] S. Bandi,[1] S. Mehta,[2] D. A. Schiraldi,[1] A. Hiltner,[1] E. Baer[1]

[1]*Department of Macromolecular Science and Engineering, Center for Applied Polymer Research, Case Western Reserve University, Cleveland, Ohio 44106*
[2]*INVISTA, 1551 Sha Lane, Spartanburg, South Carolina 29304*

ABSTRACT: Compatibilized blends of poly(ethylene terephthalate) (PET) with an aromatic polyamide such as poly(*m*-xylylene adipamide) (MXD6) have good transparency (*T*) because the constituent refractive indices (RIs) match closely. However, haziness is observed when the blends are stretched. This study demonstrated that stretching imparted a greater RI anisotropy to PET than to the aromatic polyamide. The resulting RI mismatch was responsible for the loss in *T*. Analysis of the strain-dependent birefringence revealed that different molecular deformation models described the intrinsic birefringence of the PET and aromatic polyamides. Hydrogen bonding of the polyamide may have been responsible for the difference. On the basis of these results, three approaches for improving *T* of stretched PET blends were attempted. Blends with a lower molecular weight MXD6 exhibited slightly higher *T* after stretching; however, they did not compare with stretched PET. Increasing the amount of compatibilizer reduced the particle size; however, the dimension of even the smallest particles exceeded the quarter wavelength after biaxial stretching transformed the spherical particles into platelets. Copolyamides based on MXD6 that incorporated isophthalate were designed to increase the RI of the polyamide and thereby reduce the RI mismatch with stretched PET. Unexpectedly, the poor *T* of stretched copolyamide blends was attributed to the high glass-transition temperature of the copolyamide, which hampered the molecular orientation. © 2005 Wiley Periodicals, Inc. J Appl Polym Sci 99: 225–235, 2006

Key words: blends; orientation; transparency

INTRODUCTION

Aromatic polyamides are known to possess excellent gas-barrier properties, even at high relative humidities (RHs).[1] This characteristic has been exploited with multilayered containers of poly(ethylene terephthalate) (PET) and poly(*m*-xylylene adipamide) (MXD6) that exhibit enhanced barrier properties over PET. Good transparency (*T*) is another important property of PET for packaging applications, and this feature is generally maintained in multilayered structures. However, multilayering requires special equipment to process the preforms and possibly surface treatment to improve interfacial strength and prevent delamination.

Conventional blending offers an alternative economic route for improving gas-barrier properties. Recently, improved gas-barrier properties of PET have been obtained by the blending of PET with MXD6 or with another aromatic copolyamide based on MXD6, in which 12 mol % of adipamide has been replaced with 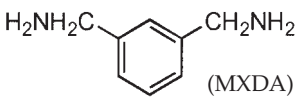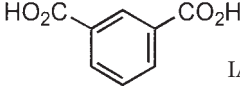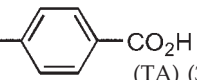isophthalamide.[2,3] In biaxially oriented films, blends with 10 wt % polyamide had their oxygen permeability reduced by a factor of up to 3.2 over that of PET when measured at 43% RH. Biaxial orientation transformed spherical polyamide domains into platelets arrayed in the plane of the film. An enhanced barrier arose from the increased tortuosity of the diffusion pathway due to the high aspect ratio of the polyamide platelets. Before orientation, the blends had good *T* due to a refractive index (RI) match between PET and the polyamide. However, haziness was observed in oriented blend films and in bottle walls blown from blends of PET with polyamides.[4,5]

In this study, we examined the origin of the haze in blends of PET with aromatic polyamides, with emphasis on the effect of stretching. The intrinsic birefringence (Δn_o) of PET and aromatic polyamides was determined and tested against various models. On the basis of these results, approaches for improving *T* of stretched PET blends were formulated that focused on decreasing the molecular weight of MXD6, increasing the compatibilizer content of the blend, and copolymerizing MXD6 with isophthalamide.

EXPERIMENTAL

PET and a copolymer in which 2.29 mol % of the terephthalate was replaced by sodium 5-sulfoisoph-

TABLE I
Chemical Structures of the Aromatic Polyamides

Polyamide	Diamine	Diacid	Dry T_g (°C)	RI
MXD6	H_2NH_2C — / — CH_2NH_2 (MXDA)	$HO_2C(CH_2)_4CO_2H$ AA	84	1.5773
MXD6-12I	MXDA	HO_2C — / — CO_2H IA (12%) + AA (88%)	93	1.5877
MXD6-18I	MXDA	IA (18%) + AA (82%)	98	1.5885
MXD6-41I	MXDA	IA (41%) + AA (59%)	106	1.5968
MXDI	MXDA	IA	166	1.6381
6IT	$H_2N(CH_2)_6NH_2$ HMDA	IA (67%) + HO_2C — / — CO_2H (TA) (33%)	125	1.5864
6IAA	HMDA	IA (29%) + AA (42%) + Azelaic acid (29%)	96	1.5656

MXDA, m-xylylene diamine; HMDA, hexamethylene diamine; IA, isophthalic acid; TA, terephthalic acid.

thalate (SIPE; to form PET-co-SIPE) were supplied as pellets by INVISTA (Spartanburg, SC). The intrinsic viscosities of the PET and PET-co-SIPE pellets were 0.84 and 0.56 dL/g, respectively, as measured at 25°C in dichloroacetic acid solution. MXD6 [number-average molecular weight (M_n) = 16,500] was supplied as pellets by Mitsubishi Gas Chemical America, Inc (New York, NY).

A copolyamide based on poly(hexamethylene isophthalamide) (6I) in which 33 mol % isophthalamide was replaced with terephthalamide (6IT) and a terpolyamide based on 6I in which 71 mol % isophthalamide was replaced with 42 mol % adipamide and 29 mol % azelamide (6IAA), were supplied by EMS Chemie (Sumter, SC). The thermal properties of MXD6, 6IT, and 6IAA were described previously.[1]

Low-molecular-weight poly(m-xylylene adipamide) (LMXD6; M_n's = 6000 and 9800) was synthesized in our laboratory as follows: 59.5 g (1.22 mol) of adipic acid (AA) was added to 70 g of water and stirred under nitrogen for 30 min at ambient temperature; this was followed by the addition 54.4 g (1.20 mol) of m-xylylene diamine (MXDA). The temperature was raised to 110°C and held constant for 2 h. After the water was distilled off from the reaction mixture, the temperature was raised to 275°C over the next 2 h, and at 275°C, it was held constant for 0.5 h. The reaction mixture became viscous, and no further distilled product was collected. A yellowish viscous liquid was collected and quenched to obtain LMXD6.

Copolyamides in which 12, 18, and 41 mol % adipamide in MXD6 were replaced with isophthalamide were designated as MXD6–12I, MXD6–18I, and MXD6–41I, respectively. The MXD6–12I was supplied by EMS Chemie. We synthesized the MXD6–18I, MXD6–41I, and poly(m-xylylene isophthalamide) (MXDI) in our laboratory by following the procedure used for LMXD6 and by changing the acid ratio in the feed. For example, to prepare MXD6–18I, we added

1.22 mol of acid [0.22 mol of isophthalic acid (IA) and 1.00 mol of AA] to 70 g of water and then added 1.20 mol of MXDA.

The composition of the polyamides and the molecular weight of LMXD6 were determined by ^{1}H-NMR with a 300-MHz Varian (Gemini 2000) Fourier transform NMR spectrometer (Palo Alto, CA). The polyamides were dissolved in d-trifluoroacetic acid (Aldrich, St. Louis, MO). The NMR spectra were run at ambient temperature. The error was ±3%. The chemical structures and designations of the polyamides are summarized in Table I.

The PET, MXD6, MXD6–12I, and 6IT pellets were dried at 120°C for 48 h in vacuo, and LMXD6, MXD6–18I, MXD6–41I, 6IAA, and the compatibilizer (PET-co-SIPE) were dried at 80°C in vacuo before blending. The pellets were dry blended and extruded in a Haake Rheomex TW-100 twin-screw extruder (Karlsruhe, Germany) with partial intermeshing, counterrotating, and conical screws with converging axes. The average screw diameter was 25.4 mm, and the average length-to-diameter ratio was 13/1. A barrel temperature of 285°C and a screw speed of 15 rpm were used. The melted blends were extruded through a 3-mm die, quenched in air, and pelletized. The possibility of a transamidation reaction between PET and MXD6 was eliminated by ^{13}C-NMR analysis, as described in a previous publication.[2] Blends were prepared with PET, 5 or 10 wt % polyamide, and various amounts of PET-co-SIPE. Transesterification during melt blending completely randomized PET and PET-co-SIPE to produce a homogeneous matrix copolymer. The blends were designated as follows: weight percentage of PET-(molar percentage of SIPE in the matrix)/weight percentage of polyamide.

The pellets were dried in vacuo for 24 h at 80°C and compression-molded between Kapton sheets in a press at 270°C to obtain films that were 0.20, 0.40, and 0.60 mm thick. The plates were heated in the press for
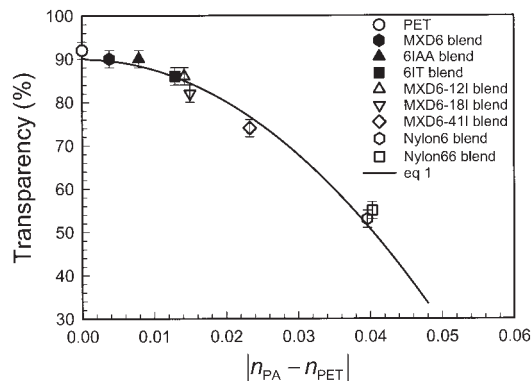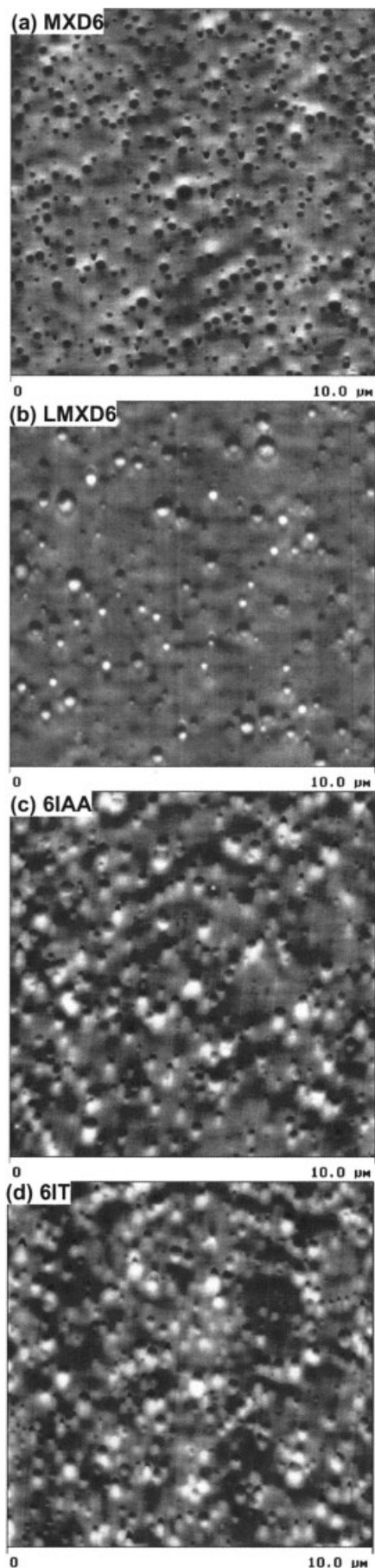
Figure 1 AFM height images of quenched PET(SIPE)/polyamide 90(0.38)/10 blends: (a) MXD6, (b) LMXD6, (c) 6IAA, and (d) 6IT.

Figure 2 T of quenched PET blends with 10 wt % polyamide as a function of RI mismatch between PET and polyamide.

4 min with repeated application and release of pressure to remove air bubbles and held at 309 psi (2.1 MPa) for an additional 4 min. Quenching from the isotropic melt into ice water produced essentially amorphous films.

Compression-molded films were conditioned at 43% RH and uniaxially or sequentially biaxially stretched in the environmental chamber of an Instron machine (Norwood, MA) at a rate of 20% min^{-1}. For constrained uniaxial stretching, a compression-molded film 150 mm wide, 40 mm long, and 0.40 mm thick was stretched at 75°C to a target draw ratio (λ) of 4. For sequential biaxial stretching, a compression-molded film 150 mm wide, 40 mm long, and 0.60 mm thick was stretched uniaxially at 75°C to a target λ of 4, remounted in the grips at 90° to the first stretch, and stretched again at 78°C to achieve a target balanced biaxial λ of 2.7 × 2.7. Grids were marked on the specimen to measure λ. After drawing, the film was rapidly cooled to ambient temperature. Some compression-molded films were immersed in water before orientation.

Twelve-ounce carbonated soft drink bottles made from PET and PET blends were supplied by INVISTA. The bottles were blown from preforms with a commercial blow-molding machine (Sidel) (Norcross, GA) after the bottle performs were stored in ambient conditions overnight. The side wall temperatures were nominally 90°C. The blowing cycle time was 3 s. The wall section was cut from the bottle for subsequent characterization.

Thermal analysis was conducted with a PerkinElmer Pyris-1 (Boston, MA) calibrated with indium and tin. Heating scans were performed under

TABLE II
T of PET and Quenched 90(0.38)/10[a] Blends

Material[b]	$|n_{PA} - n_{PET}|$	T (%)
PET	—	92
MXD6 blend	0.0038	90
6IAA blend	0.0079	90
6IT blend	0.0129	86

[a] PET(SIPE)/polyamide.
[b] Film thickness = 0.20 mm.

nitrogen at 10°C/min over a temperature range from 30 to 270°C.

Blend morphology was examined with atomic force microscopy (AFM) with a Nanoscope IIIa MultiMode head from Digital Instruments (Santa Barbara, CA) in the tapping mode. Specimens were microtomed at ambient temperature to expose their bulk morphologies.

The RIs of the polyamide films were measured with a Metricon 2010 prism coupler (Pennington, NJ) at 632.8 nm, 23°C, and 43% RH. The percentage light transmittance (±2%) was measured in accordance to ASTM D 1746 with an ultraviolet–visible spectrometer (Ocean Optics, Dunedin, FL) at 630 nm and 23°C. The film thicknesses for T measurements were about 0.20, 0.10, and 0.09 mm for the quenched, uniaxially stretched, and biaxially stretched films, respectively. The haze of bottle walls was measured in accordance with ASTM D 1003-95 at 23°C.

RESULTS AND DISCUSSION

Blends of PET with polyamides

The morphology of quenched PET blends with 10 wt % polyamide is shown in Figure 1. Spherical polyamide particles were dispersed in a continuous PET matrix. Compatibilization resulted in good dispersion of the polyamide as particles about 0.3 μm in diameter. Compatibilization by SIPE was attributed to

strong interaction between sulfonate anions and amide N—H groups.[6]

The RI of MXD6 was 1.5773. Polyamide 6IAA had a slightly lower RI of 1.5656 due to its lower aromatic comonomer content. Polyamide 6IT had a somewhat higher RI of 1.5864 because of its increased aromatic character. All had RIs relatively close to that of PET (1.5735). If a RI mismatch is sufficiently small, the Raleigh–Gans–Debye theory adequately describes light scattering from a dispersion of micrometer-size spherical particles.[7,8] For given particle size, particle concentration, and film thickness, T is inversely proportional to the square of the RI difference $(n_{PA} - n_{PET})$,[2] where n_{PA} and n_{PET} are the refractive indices of polyamide and poly(ethylene terephthalate), respectively. The T's of the 10 wt % polyamide blends are plotted versus $|n_{PA} - n_{PET}|$ in Figure 2. Data for the PET blends with 10 wt % nylon 6 and nylon 66,[9] which had larger RI mismatches with PET, are included to show the general correlation. The solid line describes the decrease in T with $(n_{PA} - n_{PET})^2$ as

$$T(\%) = -24.6 \times 10^3 \times (n_{PA} - n_{PET})^2 + 90.2 \quad (1)$$

in accordance with the Raleigh–Gans–Debye theory. As a consequence of the close RI match, the compatibilized blends of PET with MXD6 and 6IAA were almost as transparent as PET. The blend with 6IT was slightly less transparent because of the larger RI mismatch (Table II).

T of the stretched blends

One might have expected the blends to retain good T, or to even become more transparent, as they became thinner with stretching. This was not the case. In contrast to PET, which remained highly transparent after stretching, T of the polyamide blends was seriously compromised. Stretching a blend with 10 wt % polyamide to $\lambda = 4$ decreased light transmission to 66% with MXD6, 65% with 6IAA, and 45% with 6IT,

TABLE III
RI and T Values of Uniaxially Stretched PET, MXD6, and 90(0.38)/10[a] Blends Equilibrated at 43% RH Before Stretching

Material[b]	Polyamide T_g at 43% RH (°C)	RI		Unpolarized light T (%)	Polarized light	
		$n_{\parallel}$	$n_{\perp}$		$T_{\parallel}$ (%)	$T_{\perp}$ (%)
PET	—	1.6863	1.5529	89	89	89
MXD6	—	1.6103	1.5682	—	—	—
MXD6 blend	48	$\Delta n_{\parallel} = 0.0760$	$\Delta n_{\perp} = 0.0153$	66	46	81
6IAA blend	55	—	—	65	46	78
6IT blend	80	—	—	45	34	58

[a] PET(SIPE)/polyamide.
[b] Film thickness = 0.10 mm; λ = 4.
$\Delta n_{\parallel}$, difference in $n_{\parallel}$ of PET and MXD6; $\Delta n_{\perp}$, difference in $n_{\perp}$ of PET and MXD6.
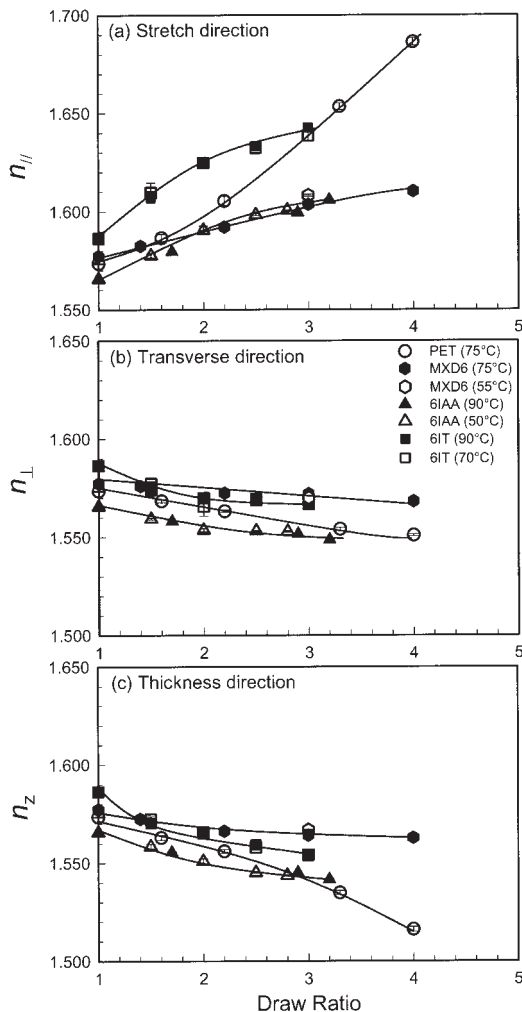
Figure 3 RI as a function of constrained uniaxial λ for PET and polyamides: (a) $n_{\parallel}$, (b) $n_{\perp}$, and (c) n_Z.

whereas stretching PET decreased light transmission only to 89%. Light transmission measured with unpolarized light is the average of the transmission in the directions parallel and perpendicular to stretching as measured with polarized light. The loss of T in the blend was predominantly due to loss in the parallel direction (Table III).

Uniaxial stretching transforms spherical MXD6 particles into elongated ellipsoids, and biaxial stretching further deforms them into flat platelets.[2,3] Although the particle size in the film plane increases significantly as a result, particle size should not have such a profound effect on T if the RI match is maintained. The reason for the reduced T of the polyamide blends may have been that stretching increased the RI mismatch between PET and the polyamide.[5] The effect of stretching on the RIs of PET and the polyamides is compared in Figure 3. Varying the stretch temperature in the vicinity of the glass-transition temperature (T_g) did not affect the polyamide RI. Reportedly, decreasing the draw temperature has tended to increase the RI of PET in the orientation direction.[10,11] Nevertheless, the temperature effect was small.

Uniaxial stretching increased the refractive index in the stretch direction ($n_{\parallel}$) and decreased the refractive index in the transverse direction ($n_{\perp}$) and the refractive index in the thickness direction (n_Z). However, the rate of change in RI with λ was much larger for PET than for the polyamides, which caused the RI difference with MXD6 and 6IAA, particularly in the stretch direction, to become larger as λ increased. The dramatic increase in the $n_{\parallel}$ mismatch of MXD6 and 6IAA accounted for the loss of blend transparency in the stretch direction ($T_{\parallel}$). In contrast, the results shown in Figure 3 for stretched 6IT suggest that this polyamide should have had a good RI match with stretched PET. The unexpectedly low T of the stretched blend was attributed to poor orientation of the small polyamide particles as a consequence of their high T_g.

A second stretch in the direction normal to the first stretch slightly increased the MXD6 blend T from 66 to 70, as measured with unpolarized light (Table IV). The second stretching reduced the refractive index mismatch between PET and MXD6 in the first stretch direction ($n_{\parallel,1}$) from 0.0760 to 0.0130 but increased the refractive index mismatch in the second stretch direc-

TABLE IV
RI and T Values of Biaxially Stretched PET, MXD6, and a 90(0.38)/10[a] Blend Equilibrated at 43% RH Before Stretching

	RI		Unpolarized light	Polarized light	
Material[b]	$n_{\parallel,1}$[c]	$n_{\parallel,2}$[d]	T (%)	$T_{\parallel,1}$[c] (%)	$T_{\parallel,2}$[d] (%)
PET[c]	1.5984	1.6360	89	91	88
MXD6[d]	1.5854	1.5913	—	—	—
MXD6 blend	$\Delta n_{\parallel,1} = 0.0130$	$\Delta n_{\parallel,2} = 0.0447$	70	72	66

$T_{\parallel,1}$, transparency parallel to the first draw; $T_{\parallel,2}$, transparency parallel to the second draw; $\Delta n_{\parallel,1}$, difference in $n_{\parallel,1}$ of PET and MXD6; $\Delta n_{\parallel,2}$, difference in $n_{\parallel,2}$ of PET and MXD6.
[a] PET(SIPE)/polyamide.
[b] Film thickness = 0.09 mm.
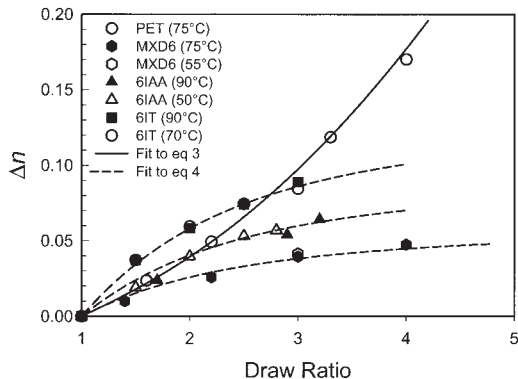[c] $\lambda = 2.7 \times 2.7$
[d] $\lambda = 2.7 \times 2.4$

Figure 4 Birefringence of PET and polyamides as a function of constrained uniaxial ratio.

tion ($n_{\|,2}$) from 0.0153 to 0.0447. A higher mismatch in the second draw direction accounted for the lower T in that direction.

The relationship between optical anisotropy or birefringence and molecular orientation is described as

$$\Delta n = \Delta n_o \langle P_2 \rangle \tag{2}$$

where Δn is the observed birefringence, which is defined as the RI difference between the stretch and thickness directions ($n_\| - n_Z$); Δn_o is the intrinsic birefringence, which is defined as Δn for perfect orientation; and $\langle P_2 \rangle$ is the orientation parameter, or Hermans function.[12] The chemical structure determines Δn_o; it can be obtained experimentally by extrapolation or estimated by the additivity of bond polarizabilities.

Two theoretical approaches for the prediction of Δn_o have been proposed: the affine and pseudoaffine deformation models.[12–14] In the affine model, network junctions are thought to be connected by flexible chains. On stretching, the network points are displaced in direct proportion to the macroscopic deformation. Consequently, the rotatable random links comprising the network chains gradually adopt a more and more oriented configuration. For this type of rubber-like deformation, the orientation parameter ($\langle P_2 \rangle$) can be described as

$$\langle P_2 \rangle = \frac{\Delta n}{\Delta n_o} = \frac{1}{5N}\left(\lambda^2 - \frac{1}{\lambda}\right) \tag{3}$$

where N is the number of random links between the network points and λ.

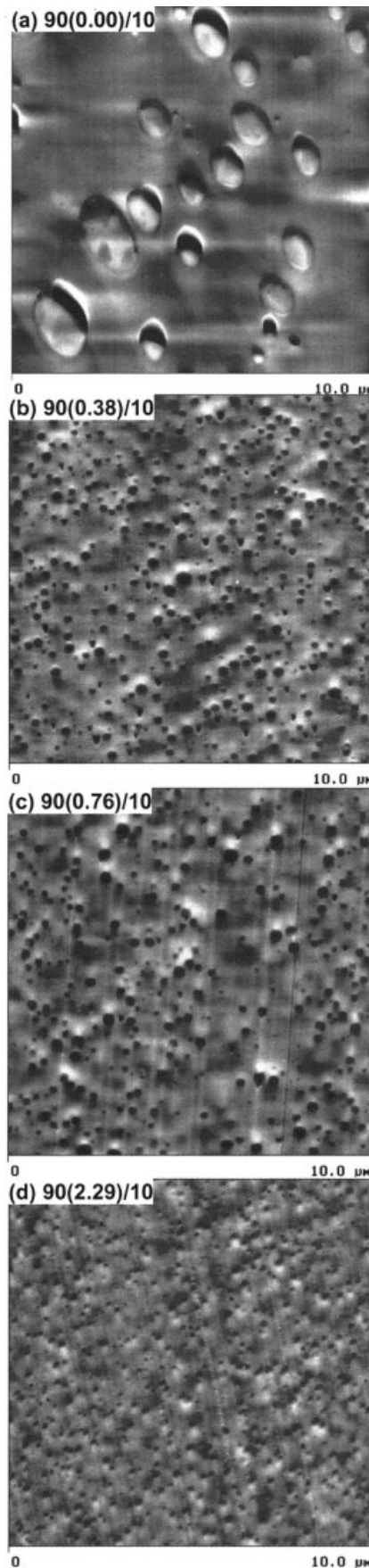In pseudoaffine deformation, on the other hand, the structural elements undergoing deformation are as-

Figure 5 AFM height images of quenched PET(SIPE)/MXD6 blends: (a) 90(0.00)/10, (b) 90(0.38)/10, (c) 90(0.76)/10, and (d) 90(2.29)/10.

TABLE V
Effect of the Compatibilizer Content on *T* of the MXD6 Blends

Material	Domain size (μm)	T (%)			Platelet dimension	
		Quenched	Uniaxially stretched	Biaxially stretched	L (μm)	W (nm)
PET	—	92	89	89	—	—
90(0.00)/10[a]	2.0	85	30	12	5.4	80
90(0.38)/10[a]	0.3	90	66	70	0.81	27
90(0.76)/10[a]	0.3	90	70	75	0.81	27
90(2.29)/10[a]	0.2	89	68	77	0.54	18

[a] PET(SIPE)/MXD6.

sumed to have no extensibility themselves but are rigid entities that simply rotate in proportion to the macroscopic deformation. This leads to the expression

$$\langle P_2 \rangle = \frac{\Delta n}{\Delta n_o}$$
$$= \frac{1}{2}\left(\frac{2\lambda^3 + 1}{\lambda^3 - 1} - \frac{3\lambda^3}{(\lambda^3 - 1)^{3/2}} \arctan(\lambda^3 - 1)^{1/2} \right) \quad (4)$$

The birefringence of PET drawn at 75°C and the polyamides drawn at various temperatures are shown as a function of uniaxial λ in Figure 4. The slightly concave shape of the PET curve suggests that the orientation of the PET films followed the affine deformation model. This was consistent with various studies of melt-spun PET fibers and PET films drawn above T_g.[15–17] The solid line represents the fit of eq. (3) with $N = 4$, which gave a Δn_o of 0.224, in good agreement with literature values of 0.21–0.24 for amorphous and crystalline PET.[18,19] The convex shape of the polyamide curves indicated that orientation followed the pseudoaffine model. The experimental data were satisfactorily described by eq. (4), with Δn_o values of 0.060, 0.094, and 0.135 for MXD6, 6IAA, and 6IT, respectively, independent of the stretching temperature. Reportedly, nylon 6 fibers also follow the pseudoaffine model regardless of spinning temperature and rate.[13] It may be that this is a general characteristic of polyamides caused by the hydrogen-bonding network.

The high Δn_o of PET (0.224) was attributed to the linear configuration of the backbone aromatic ring, which on orientation, contributes substantially to the polarizability in the parallel direction. Similarly, 6IT had the highest Δn_o (0.135) of the polyamides due to 33 mol % terephthalamide in the repeat unit. On the other hand, metasubstitution of the aromatic group hindered the linear orientation of the molecules, which led to the lowest Δn_o (0.060) for MXD6. This was even lower than the Δn_o values of nylon 6 (0.067–0.089).[20] On the basis of these results, several approaches were used to improve *T* of the stretched blend.

Effect of the compatibilizer content

Without compatibilizer, the blend morphology consisted of relatively large spherical or ellipsoidal polyamide particles dispersed in a continuous PET matrix. The relatively coarse morphology with particles as large as 2 μm confirmed the incompatibility of the two constituents [Fig. 5(a)]. The whitening of uncompatibilized MXD6 blends during stretching suggested that interfacial failure was responsible for the exceptionally poor *T* (Table V).

One approach to the improvement of *T* was to enhance the interfacial adhesion and reduce the domain size by an increase in the compatibilizer content. The addition of 0.38 and 0.76 mol % SIPE to the PET phase reduced the MXD6 particle size to 0.3 μm [Fig. 5(b,c)]. Increasing SIPE content further to 2.29 mol % reduced the particle size somewhat more to 0.2 μm [Fig. 5(d)].

Because of the close RI match between MXD6 and PET, particle size had only a small effect on *T* of the unoriented blends. *T* increased from 85% for the uncompatibilized blend to 90% for the compatibilized blends compared to 92% for PET (Table V). However, even the lowest compatibilizer level increased *T* of stretched blends from 30 to 66% after uniaxial stretch-
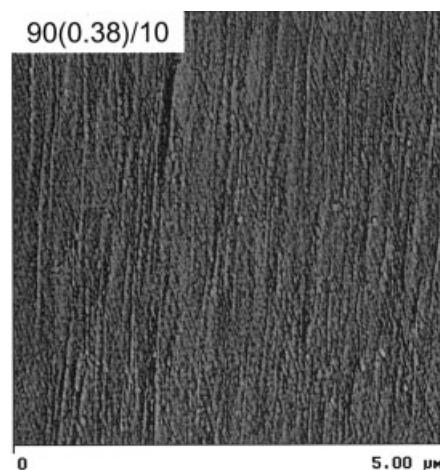

Figure 6 AFM phase image of the biaxially stretched PET-(SIPE)/MXD6 90(0.38)/10 blend.
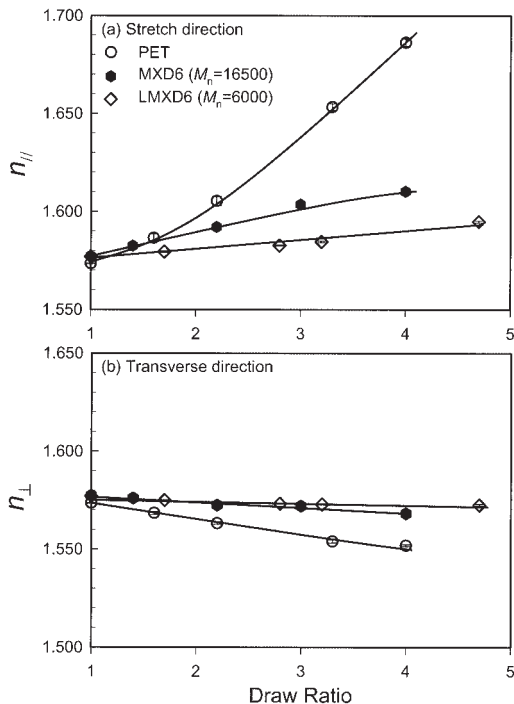
Figure 7 RI as a function of constrained uniaxial λ for PET, MXD6, and LMXD6: (a) $n_{\parallel}$ and (b) $n_{\perp}$.

ing and from 12 to 70% after biaxial stretching. Probably, the smaller particle size and enhanced interfacial adhesion prevented voiding. Increasing compatibilizer further improved T somewhat more, but even with the highest compatibilizer level, T of the stretched blend was much lower than T of stretched PET as a consequence of RI mismatch.

Stretching transformed the spherical polyamide domains into thin platelets oriented in the plane of the film (Fig. 6). With the assumption that spherical domains are deformed into circular platelets of equal volume, the thickness (W) and diameter (L) of the platelets can be estimated according to

$$\frac{4}{3}\pi r^3 = \pi(\lambda r)^2 W = \pi\left(\frac{L}{2}\right)^2 W \qquad (5)$$

TABLE VI
Effect of MXD6 Molecular Weight on T of 90(0.38)/10[a] Blends

Material	$\lvert n_{PA} - n_{PET} \rvert$	Quenched T (%)	Uniaxially stretched T (%)	Biaxially stretched T (%)
PET	—	92	89	89
MXD6 blend	0.0038	90	66	70
LMXD6 blend ($M_n = 6000$)	0.0035	92	67	75

[a] PET(SIPE)/polyamide.

TABLE VII
T and Haze of 12-oz. Blend Bottle Walls

Bottle wall composition[a]	T (%)	Haze (%)
100(0)/0	93	5.72
100(0.15)/0	91	5.63
95(0.15)/5 MXD6	80	10.80
95(0.15)/5 LMXD6 ($M_n = 9800$)	82	9.24

Bottle wall thickness = 0.30 mm.
[a] PET(SIPE)/polyamide.

where r is the radius of the spherical domains before stretching and λ is the balanced biaxial draw ratio of 2.7. The values of L and W from eq. (5) are listed in Table V. The dimensions were consistent with the platelet size observed in stretched blends by AFM.

The calculated W for the compatibilized blends was well below the quarter wavelength (150 nm), in which case the Rayleigh scattering could be ignored. However, the lateral dimensions of the platelets were comparable to or larger than the quarter wavelength. This was the source of the light scattering. To reduce L in 2.7×2.7 biaxially oriented films below 150 nm, the particle size in unoriented blends must be smaller than 0.05 μm. This did not appear feasible, and other approaches were required.

Effect of LMXD6

It was reported that LMXD6 ($M_n < 15{,}000$) reduced the haze of biaxially oriented PET blends by a factor of 2–5 compared to blends with high-molecular-weight MXD6 ($M_n = 26{,}000$), without a significant loss in oxygen permeability.[21] Therefore, LMXD6 was included in this study. $n_{\parallel}$ and $n_{\perp}$ for LMXD6 ($M_n = 6000$), MXD6 ($M_n = 16{,}500$), and PET drawn at 75°C are plotted in Figure 7 as a function of uniaxial λ.
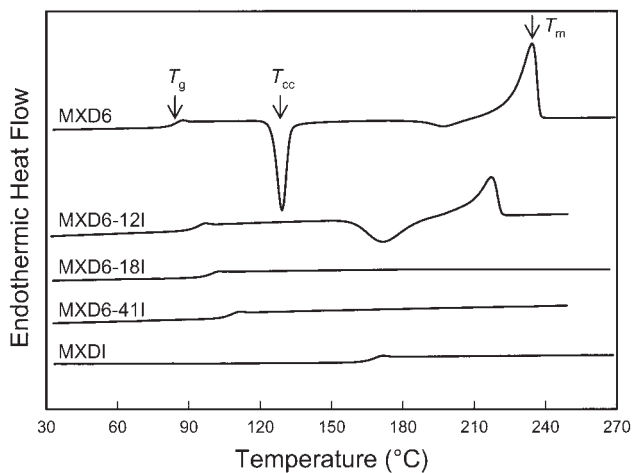

Figure 8 Thermal analysis of quenched, dry copolyamides.

TABLE VIII
Properties of Dry PET, MXDI, and Copolymers

Polymer	T_g (°C)	T_{cc} (°C)	ΔH_{cc} (J/g)	T_m (°C)	ΔH_m (Jg)
PET	78	139	35	247	41
MXD6	84	129, 200	40, 7	235	55
MXD6-12I	93	173	22	218	22
MXD6-18I	98	—	—	—	—
MXD6-41I	106	—	—	—	—
MXDI	166	—	—	—	—

ΔH_{CC}, heat of cold crystallization; ΔH_m, heat of melting.

Although LMXD6 could be extended to a higher λ, the change in RI with λ was much flatter for LMXD6 than for MXD6. The low birefringence of stretched LMXD6 was attributed to disentanglement and chain slippage during extension.

Molecular weight did not affect the RI of MXD6, and consequently, quenched blends of PET with LMXD6 and MXD6 were equally transparent. However, after stretching, the LMXD6 blend was slightly more transparent than the MXD6 blend (Table VI). The same trend was observed in 12-oz. bottle walls. Bottles blown from blends with lower molecular weight MXD6 (M_n = 9800) had a slightly higher T and a slightly lower haze than bottles blown from blends with higher molecular weight MXD6 (Table VII). However, the haze reduction was considerably less than reported previously.[21]

According to the results presented in Figure 7, the $n_\parallel$ mismatch in stretched blends of PET and LMXD6 should have been larger than the mismatch between PET and MXD6, which would have resulted in a lower T of the stretched LMXD6 blend. The fact that the stretched LMXD6 blend was slightly more transparent than the MXD6 blend was not due to smaller particle size, as the particle sizes were essentially the same (see Fig. 1). Evidently, the optical properties of the stretched LMXD6, as presented in Figure 7, did not duplicate the optical properties of the stretched LMXD6 particles in the blend. The interaction of LMXD6 with the compatibilizer may have inhibited disentanglement and promoted the orientation of LMXD6 in small particles. It was also possible that LMXD6 particles possessed a more diffuse interphase than higher molecular weight MXD6 particles, and this contributed to the slightly better T.

Copolymers of MXD6 with isophthalamide

Another approach to increasing T of stretched blends was aimed at modifying MXD6 to increase n_{PA} and, thereby, achieving a closer RI match between stretched PET and stretched polyamide. The target n_{PA} was estimated to be about 1.600 to achieve $n_\parallel$ match with PET at λ of 2.7, provided that Δn_o did not
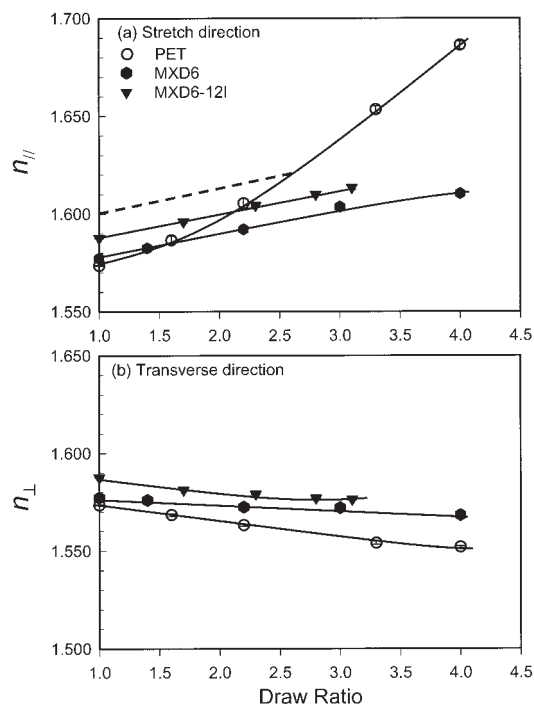

Figure 9 RI as a function of uniaxial λ for PET, MXD6, and MXD6–12I: (a) $n_\parallel$ and (b) $n_\perp$. The dashed line in (a) describes a polyamide with a $n_\parallel$ value matching that of PET at λ = 2.7.

change substantially. It was anticipated that a polyamide with n_{PA} of 1.600 would produce a hazy blend but that the blend would become clear when stretched. To achieve n_{PA} of 1.600, adipamide in MXD6 was partially replaced with isophthalamide.

The heating thermograms of dry copolyamide films are shown in Figure 8. T_g increased with isophthalamide content from 84°C for MXD6 to 166°C for MXDI (Table VIII). The effect of copolymerization was reflected in a higher cold crystallization temperature (T_{cc}), a lower melting temperature (T_m), and a lower heat of melting for MXD6–12I compared to MXD6. Thermograms of MXD6–18I, MXD6–41I, and MXDI showed no crystallization or melting. The T_g's, the peak T_{cc} and T_m, and their enthalpies are compiled in Table VIII.

As expected, n_{PA} of the copolyamide increased with isophthalamide content due to increased aromaticity.

TABLE IX
T of Quenched 90(0.38)/10[a] Blends

Material[b]	$\|n_{PA} - n_{PET}\|$	T (%)
PET	-	92
MXD6 blend	0.0038	90
MXD6-12I blend	0.0142	85
MXD6-18I blend	0.0150	82
MXD6-41I blend	0.0233	74

[a] PET(SIPE)/polyamide.
[b] Film thickness = 0.20 mm.

TABLE X
T of 90(0.38)/10[a] Blends Equilibrated at 43% RH Before Stretching

| Material | Polyamide T_g at 43% RH (°C) | Uniaxially stretched | | | Biaxially stretched |
| | | Unpolarized light *T* (%) | Polarized light | | Unpolarized light *T* (%) |
			$T_{\parallel}$ (%)	$T_{\perp}$ (%)	
PET	—	89	89	88	89
MXD6 blend	48	66	46	81	70
MXD6-12I blend	55	56	46	64	72
MXD6-18I blend	64	52	42	62	69
MXD6-41I blend	70	52	42	64	56

[a] PET(SIPE)/polyamide.

The effect of stretching on $n_{\parallel}$ and $n_{\perp}$ of MXD6–12I is shown in Figure 9. The slightly convex shape of the $n_{\parallel}$ curves indicated that orientation of the copolyamide followed the pseudoaffine deformation model. The experimental data for MXD6–12I were satisfactorily described by eq. (4) with $\Delta n_o = 0.064$. The increase in n_{PA} resulted in a closer match with PET in $n_{\parallel}$ but a larger mismatch in $n_{\perp}$. Compression-molded films of MXD6–18I and MXD6–41I were brittle because of their low molecular weight and could not be stretched.

Compatibilized blends of PET with 10 wt % copolyamide showed excellent dispersion of 0.3 μm particles. *T* of the quenched blends decreased from 90% for the MXD6 blend to 74% for the MXD6–41I blend due to the increasing RI mismatch between PET and the polyamide (Table IX). *T* of the quenched blends was adequately described by eq. (1) (see Fig. 2).

When they were uniaxially stretched at 43% RH, contrary to expectations, *T* values of the copolyamide blends were even lower than *T* of the MXD6 blend (Table X). This was primarily due to lower transparency in the transverse direction ($T_{\perp}$). A larger mismatch in $n_{\perp}$ (see Fig. 9) reduced $T_{\perp}$; however, a closer match in $n_{\parallel}$ did not increase $T_{\parallel}$. After biaxial stretching, the *T* values of the MXD6–12I and MXD6–18I blends were about the same as that of the MXD6 blend (70%); however, *T* decreased to 56% for the MXD6–41I blend.

The unexpectedly low *T* of the stretched copolyamide blends was attributed to the high T_g of the copolyamide, which hampered molecular orientation. In an attempt to lower the polyamide T_g, blends were soaked in water before stretching. This improved *T* of the stretched blends, particularly in the stretch direction (Table XI). However, this *T* was still significantly lower than that of PET.

CONCLUSIONS

Blends of PET with aromatic polyamides exhibited high gas barriers after biaxial stretching transformed the spherical polyamide particles into platelets of high aspect ratio. However, many packaging applications also require good *T*. Compatibilized blends of PET with some aromatic polyamides had good *T*'s in the unoriented glass because their RIs matched closely. Unfortunately, haziness was observed after biaxial stretching because stretching imparted greater RI anisotropy to PET than to the polyamide. Analysis of the strain-dependent birefringence revealed that different molecular deformation models described Δn_o of PET and aromatic polyamides. Hydrogen bonding of the polyamide may have been responsible for the difference. Understanding the birefringence led us to several approaches for improving *T* of stretched PET blends. Although these were partially successful, none

TABLE XI
T of 90(0.38)/10[a] Blends Saturated in Water Before Stretching

| Material | Polyamide T_g saturated (°C) | Uniaxially stretched | | | Biaxially stretched |
| | | Unpolarized light *T* (%) | Polarized light | | Unpolarized light *T* (%) |
			$T_{\parallel}$ (%)	$T_{\perp}$ (%)	
PET	—	89	89	89	91
MXD6 blend	3	72	65	77	75
MXD6-12I blend	11	—	—	—	75
MXD6-18I blend	16	71	68	77	70
MXD6-41I blend	24	75	69	79	69

[a] PET(SIPE)/polyamide.

resulted in a stretched blend that had the T of stretched PET. Blends with a lower molecular weight MXD6 exhibited a slightly higher T after stretching; however, the effect was not as large as that reported in the literature. Increasing the amount of compatibilizer reduced the particle size; however, the dimensions of even the smallest particles exceeded the quarter wavelength after biaxial stretching transformed the spherical particles into platelets. Copolymerization with isophthalamide was aimed at the increase of the RI of the polyamide and the reduction of the RI mismatch with stretched PET. The unexpectedly poor T of the stretched copolyamide blends was attributed to the high T_g of the copolyamide, which hampered molecular orientation.

References

 1. Hu, Y. S.; Mehta, S.; Schiraldi, D. A.; Hiltner, A.; Baer, E. J Polym Sci Part B: Polym Phys 2005, 43, 1365.
 2. Prattipati, V.; Hu, Y. S.; Bandi, S.; Mehta, S.; Schiraldi, D. A.; Hiltner, A.; Baer, E. J Appl Polym Sci 2005, 97, 1361.
 3. Hu, Y. S.; Prattipati, V.; Mehta, S.; Hiltner, A.; Baer, E. Polymer 2005, 46, 5202.
 4. Watanabe, T. J Plastic Film Sheeting 1987, 3, 215.
 5. Maruhashi, Y.; Iida, S. Polym Eng Sci 2001, 41, 1987.
 6. Eisenberg, A.; Kim, J.-S. Introduction to Ionomers; Wiley: New York, 1998; Chapter 9, p 267.
 7. Willmouth, F. M. In Optical Properties of Polymers; Meeten, G. H., Ed.; Elsevier: London, 1986; Chapter 5, p 265.
 8. Tse, A.; Laakso, R.; Baer, E.; Hiltner, A. J Appl Polym Sci 1991, 42, 1205.
 9. Hu, Y. S.; Mehta, S.; Hiltner, A.; Baer, E. J Appl Polym Sci, to appear.
10. Cakmak, M.; White, J. L.; Spruiell, J. E. Polym Eng Sci 1989, 29, 1534.
11. Jabarin, S. A. Polym Eng Sci 1992, 32, 1341.
12. Structure and Properties of Oriented Polymers; Ward, I. M., Ed.; Chapman & Hall: London, 1997; Chapter 1, p 1.
13. Penning, J. P.; van Ruiten, J.; Brouwer, R.; Gabriëlse, W. Polymer 2003, 44, 5869.
14. Hamza, A. A.; Sokkar, T. Z. N.; El-Farahaty, K. A.; El-Dessouky, H. M. Polym Test 2004, 23, 203.
15. Nobbs, J. H.; Bower, D. I.; Ward, I. M. J Polym Sci Polym Phys Ed 1979, 17, 259.
16. Rietsch, F.; Duckett, R. A.; Ward, I. M. Polymer 1979, 20, 1133.
17. Ward, I. M.; Bleackley, M.; Taylor, D. J. R.; Cail, J. I.; Stepto, R. F. T. Polym Eng Sci 1999, 39, 2335.
18. Garg, S. K. J Appl Polym Sci 1982, 27, 2857.
19. Huijts, R. A.; Peters, S. M. Polymer 1994, 35, 3119.
20. Balcerzyk, E.; Kozlowski, W.; Wesolowska, E.; Lewaszkiewicz, W. J Appl Polym Sci 1981, 26, 2573.
21. Turner, S. R.; Connell, G. W.; Stafford, S. L.; Hewa, J. D. U.S. Pat. 6,444,283 (2002).